

# AIM: Let Any Multi-modal Large Language Models Embrace Efficient In-Context Learning

Jun Gao<sup>\*1</sup>, Qian Qiao<sup>1</sup>, Ziqiang Cao<sup>1</sup>, Zili Wang, Wenjie Li<sup>2</sup>

Institute of Artificial Intelligence, School of Computer Science and Technology, Soochow University<sup>1</sup>  
Department of Computer Science, Hong Kong Polytechnic University, Hong Kong<sup>2\*</sup>

## ABSTRACT

In-context learning (ICL) facilitates Large Language Models (LLMs) exhibiting emergent ability on downstream tasks without updating billions of parameters. However, in the area of multi-modal Large Language Models (MLLMs), two problems hinder the application of multi-modal ICL: (1) Most primary MLLMs are only trained on single-image datasets, making them unable to read multi-modal demonstrations. (2) With the demonstrations increasing, thousands of visual tokens highly challenge hardware and degrade ICL performance. During preliminary explorations, we discovered that the inner LLM tends to focus more on the linguistic modality within multi-modal demonstrations to generate responses. Therefore, we propose a general and light-weighted framework **AIM** to tackle the mentioned problems through **A**ggregating **I**mage information of **M**ultimodal demonstrations to the dense latent space of the corresponding linguistic part. Specifically, AIM first uses the frozen backbone MLLM to read each image-text demonstration and extracts the vector representations on top of the text. These vectors naturally fuse the information of the image-text pair, and AIM transforms them into fused virtual tokens acceptable for the inner LLM via a trainable projection layer. Ultimately, these fused tokens function as variants of multi-modal demonstrations, fed into the MLLM to direct its response to the current query as usual. Because these fused tokens stem from the textual component of the image-text pair, a multi-modal demonstration is nearly reduced to a pure textual demonstration, thus seamlessly applying to any MLLMs. With its de facto MLLM frozen, AIM is parameter-efficient and we train it on public multi-modal web corpora which have nothing to do with downstream test tasks. We comprehensively evaluate AIM on various open-ended and closed-ended tasks. Results show that AIM always achieves comparable or better performance than its underlying backbone and other multi-modal baselines focusing on the multi-modal ICL scenario. Additionally, AIM significantly reduces memory costs by discarding thousands of image tokens, thereby increasing the number of allowed demonstrations from 1 to 16 within a 24G CUDA memory allocation.

## KEYWORDS

In-Context Learning, Multi-Modal Large Language Models

## 1 INTRODUCTION

In-context learning (ICL) exhibits spectacular emergent ability in the NLP community [5, 36, 41], enabling scaled-up Large Language Models (LLMs) [27, 34, 35, 37, 39, 42] to attain desirable performance on **training-agnostic** data by providing with handful in-context demonstrations. Unfortunately, primary Multi-modal

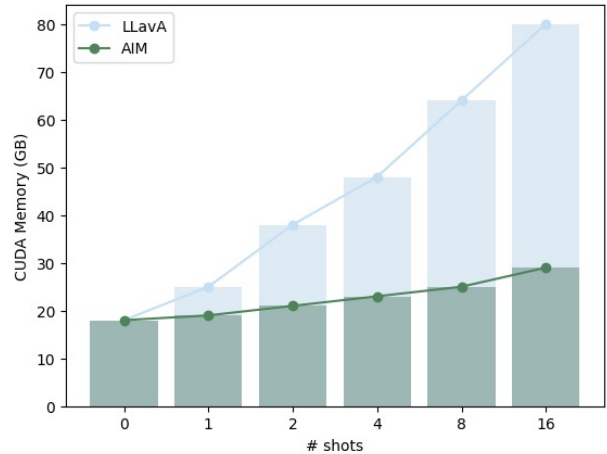


**Figure 1: Memory cost comparison between AIM and LLaVA-Next on Flickr30k. The memory cost of LLaVA-Next occurs a surge, while it almost remains unchanged in AIM.**

Large Language Models (MLLMs) such as LLaVA [20, 22], LLaMA-Adapter [45], and BLIP-2 [17], only support a single image as the vision input, impossible to learn from multi-modal demonstrations composed of <image, instruction text, reference text> pairs. Additionally, most MLLMs utilize Perceiver [1, 2, 8, 17, 20–22] to generate visual tokens from image features encoded by an existing vision encoder, assisting the inner LLM understand visual inputs. However, multiple images in multi-modal demonstrations will produce thousands of visual tokens, resulting in extreme memory costs as depicted in Figure 1. Meanwhile, the length disaster brought by multi-modal demonstrations might be one of the key factors constraining the performance of multi-modal ICL [1–3, 12, 16, 46]. Our experiments indicate a dramatic deterioration in the Perplexity (PPL) of answers generated by MLLMs with increasing demonstrations introduced (refer to Figure 5).

During the early exploration, we surprisingly found that MLLMs attend more to the linguistic modality, namely the texts in demonstrations, than the vision modality for response generation, as shown in Figure 3. This finding is in little conflict with the conclusion in textual ICL that the input is more important [7, 41]. Motivated by this finding, we propose the framework AIM, with the **aim** to make *any* MLLM embrace efficient multi-modal ICL through approximately reducing an image-text demonstration into a pure textual demonstration. In contrast to MLLMs that treat visual and textual tokens equally [3, 20, 22, 46], AIM integrates image information into the dense latent space of linguistic modality in

<sup>\*</sup>Corresponding to junegao1106@gmail.com

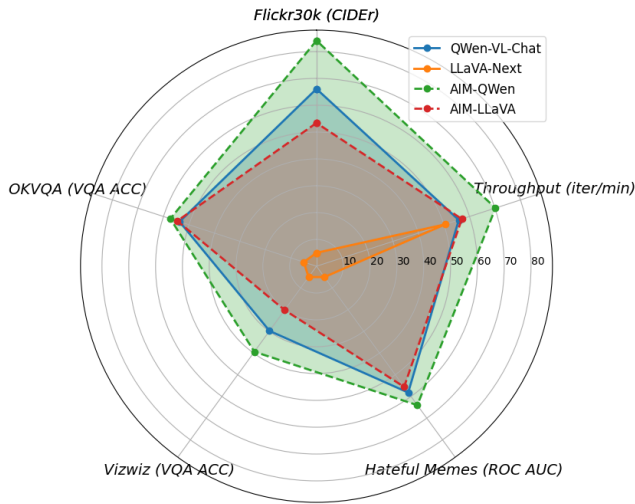


**Figure 2: Performance comparison between AIM and its underlying backbone in the 16-shot ICL setting.**

multi-modal demonstrations, leveraging the inner frozen MLLM itself. Specifically, AIM first applies the inner MLLM to forward each demonstration independently to obtain the hidden states of demonstrated text (including the instruction and the reference). Since the image information is naturally included in these hidden states [36] due to the stacked transformer layers, AIM discards the original image tokens and converts the textual hidden states to fused virtual tokens acceptable for LLMs via a trainable projection layer. Finally, the fused tokens replace the original image-text pair, serving as a text-like demonstration, fed into the inner LLM to guide response generation as normal. As textual tokens are far shorter than visual ones, AIM greatly mitigates the length disaster in multi-modal ICL, retaining less than 10% tokens compared with original multi-modal demonstrations (refer to Table 4), thereby reducing memory costs and enhancing generation efficiency. Notably, as aggregating each image information is independent, AIM supports asynchronous processing of different demonstrations within a batch or synchronous repetition of the above step for each demonstration, thus configuring a dense demonstration sequence for few-shot settings through horizontal concatenation.

AIM keeps its de facto MLLM frozen, only equipping 17M trainable parameters originating from the projection layer. Considering ICL was proposed in a low-resource setting, previous studies training models on a mixture of downstream task datasets seem inappropriate that MLLMs perhaps fall into the short-cut answer, resulting in outstanding but not solid results on involved/related tasks. Hence, following the technical report of OpenFlamingo [2], we train the projection layer on the subset of MMC4 [47], containing 223k images and 1M sequences from websites. We select LLaVA-Next and Qwen-VL as the underlying MLLM in AIM to verify the generality, representing MLLMs pre-trained on single and multi-images, respectively. Furthermore, we comprehensively evaluate AIM on captioning [30], vision question answering (VQA) [11, 24], and classification [14], none of them occurring in the mixture downstream training dataset of the underlying MLLMs. Figure 2 reveals

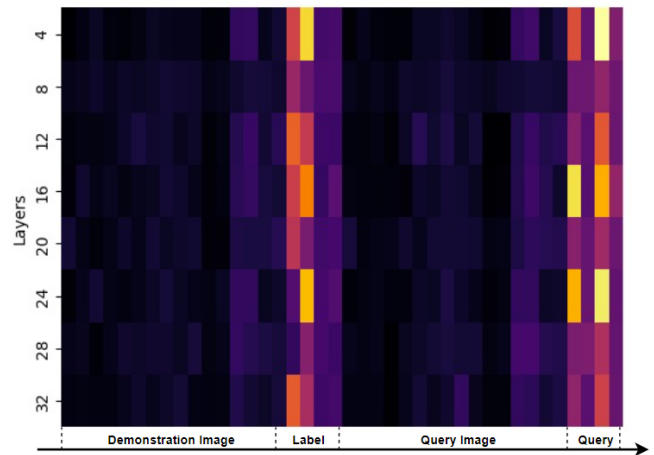


**Figure 3: The hot map of attention scores when Qwen-VL generates the first token on the hateful memes dataset. The brighter represents that responses to be generated have paid more attention to the current visual/textual tokens. Obviously, the generation relies more on the textual part of a multi-modal demonstration**

that AIM always achieves comparable or better performance than its underlying backbone and other multi-modal baselines focusing on the multi-modal ICL scenario. Additionally, AIM is far more memory-friendly than its naive backbone, thereby supporting more demonstrations and higher inference throughput. Generally, our main contributions are as follows:

- To the best of our knowledge, we are the first to analyze the attention distribution of multi-modal demonstrations during generation, revealing that MLLMs prioritize attention towards the linguistic over the visual modality in multi-modal demonstrations.
- Building upon this finding, we propose to transform multi-modal demonstrations to text-like representations, enabling any MLLMs qualified for efficient multi-modal ICL.
- Our proposed AIM exhibits efficiency in terms of trainable parameters, memory usage, and inference throughput.

## 2 RELATED WORK

### 2.1 Multi-modal Large Language Models

Recently, the development of LLMs significantly advanced the iterations of MLLMs, and the inner LLMs play crucial roles. Researchers first trained the vision encoder to align to the frozen language models [33], performing vision-language tasks. Predominate MLLMs can be abstracted to Perceiver & LLM architecture, where the Perceiver is usually composed of a Vision Transformer (ViT) [9] to extract image features and an adapter, performing vision and language alignment at the input of LLM. Specifically, the perceiver in Qwen-VL [3] and the Q-Former in BLIP-2 [17] apply learnable queries to extract visual information based on cross-attention, while the Connector in LLaVA [20–22] directly projects the visual features extracted from the pre-trained ViT-L/14 in CLIP [31]. Considering the further alignment within LLMs, Flamingo [1] introduced the

XATTN layer to align visual tokens originating from the Resampler and textual embeddings within the LLM. InternLM [44] propose Partial LoRA to align vision tokens to the LLM.

However, the perceiver in MLLM will introduce hundreds or even thousands of visual tokens to the inner LLM in ICL, resulting in over-length multi-modal prompts and thereby bringing enormous memory costs.

## 2.2 In-Context Learning

In the field of NLP, LLMs including ChatGPT [23], GPT-4 [29], and LLaMA [26], exhibit general spectacular emergent abilities on downstream tasks that provide a novel paradigm for generative models known as “Pre-training, Prompting, and Prediction”. Within this paradigm, ICL assumes a pivotal role, bolstering the generalization capability of LLMs [37, 38, 42], without necessitating billions of parameters gradient updating.

The success of ICL in NLP boosts studies focusing on transforming it into the multi-modal setting [1, 33, 43, 46]. Additionally, researchers extensively explore the influence of diverse demonstration configurations in captioning [43]. As far as we know, recent studies focusing on multi-modal ICL [1, 2, 16, 20, 46] overlook deployment challenges to some extent. Qwen-VL [3] and MMICL [46] treat visual and textual tokens equally during training, brought serious length disasters and restricted ICL performance due to introducing enormous vision tokens. Flamingo [1] treated image information as informative noises adding to textual embeddings through extra introduced adapters within selectional inner LLM layers, resulting in additional module latency. However, visual tokens of different images still share the same input window, bringing extra memory costs. LLaVA-Next [21] specialized in single-image inference, and it achieved outstanding performance on popular multi-modal benchmarks and textual-only ICL, while its excellent performance failed to extrapolate to practical multi-modal ICL settings, exhibiting poor ability of instruction following. Additionally, LLaVA-Next connected pre-trained ViT and LLM via an MLP that resulted in thousands of visual tokens for high-resolution pictures, causing more serious length disasters than perceivers based on cross-attention.

## 2.3 Efficient In-Context Demonstration

Considering the huge inference costs brought by ICL, researchers recently focused more on formulating efficient in-context demonstrations [40]. Similar to prefix tunning [18], Gist Tokens [28] were proposed to replace various task instructions. AutoCompressor [6] first randomized segmented the texts with thousands of words into model-accepted range and then recursively generated soft prompts for each segment. Similarly, ICAE [10] employed a LoRA-adopted Llama-7b [32] to compress the processed demonstrations to compact virtual tokens. Correspondingly, researchers also endeavored to shorten prompts by extracting informative tokens from the original ones [13, 19], namely token pruning [15] or token merging [4]. LLMingua [13] and Selective Context [19] shared similarities but diverged on whether to eliminate tokens with high or low PPL.

Unfortunately, these outstanding studies only focus on the textual modality, which did not suffer from the modal gap in MLLMs.

To our best known, AIM is the first to explore the construction of efficient multi-modal demonstrations.

## 3 METHODOLOGY

We propose AIM as illustrated in Figure 4, which is a training- and inference-efficient framework that aggregates image information of multi-modal demonstrations into their latent space of demonstrated text for any MLLMs. Considering different details of popular MLLMs, we present an empirical comparison in Table 1. Specifically, The Flamingo is distinguished from others by its Gated XATTN layer inserted in the LLM blocks to fuse image information into embeddings. Hence, the introduced adapter achieves a trade-off between memory costs and inference latency. LLaVA-Next directly projects visual features extracted from pre-trained ViT to thousands of visual tokens, resulting in higher memory cost increment than other methods based on Q-Former.

Notably, AIM discards substantial visual tokens in multi-modal demonstrations after aggregating demonstrated image information into demonstrated text, resembling a prompt containing a single image. Consequently, AIM operates seamlessly with any MLLMs, regardless of whether they initially understand multimodal demonstrations well. AIM employs the 7B version of Qwen-VL and LLaVA-Next as the de facto backbone to verify the transfer universality across different underlying MLLMs, representing the two coarse-grained types of MLLMs divided by training data.

### 3.1 Preliminary

A multi-modal ICL prompt encompasses several demonstrations consisting of image-text pairs ( $\langle X_1, Y_1 \rangle, \langle X_2, Y_2 \rangle, \dots, \langle X_N, Y_N \rangle$ ) and a query denoted as  $\langle X_{query}, ins. \rangle$ , where  $X_i$  and  $X_{query}$  representing the  $i$ -th demonstration image and the query image. Additionally, we use manually designed instructions  $ins.$  to wrap the bare label for each demonstration. Thus, the demonstrated texts in  $i$ -th demonstration are composed of instruction  $ins.$  and its reference label  $Y_i$ , e.g., **[IMG]** Describe the image in a sentence in English: **[Caption]**.

### 3.2 Image Information Aggregation

Taking into account our discoveries, AIM configures efficient demonstrations by disrupting the original parity between visual and linguistic modalities. AIM signals the linguistic space to gather image information via the forward propagation of the inner LLM, as illustrated in the left part of Figure 4. Practically, we split the original concatenated  $N$ -shot demonstrations into  $N$  separate image-text pairs, and decorate labels with manually designed instructions. Then, we feed images to the Perceiver, namely, the Visual Prompt Generator (VPG), to obtain the visual tokens ( $X_N^v, X_2^v, \dots, X_N^v$ ) normally. Consequently, the LLM forwards  $X_i^v$  attached with the  $i$ -th textual embeddings  $Y_i$ , obtaining last hidden states corresponding to  $Y_i$ , while dropping the others<sup>1</sup>:

$$\dots, H_i^Y = \text{Forward}(X_i^v \oplus Y_i). \quad (1)$$

Due to the inner transformer layers,  $H_i^Y$  is compelled to attend to the preceding visual tokens, making the latter textual tokens able to aggregate visual information. However,  $H_i^Y$  is still in the output

<sup>1</sup> $\oplus$  means token-level concatenation.

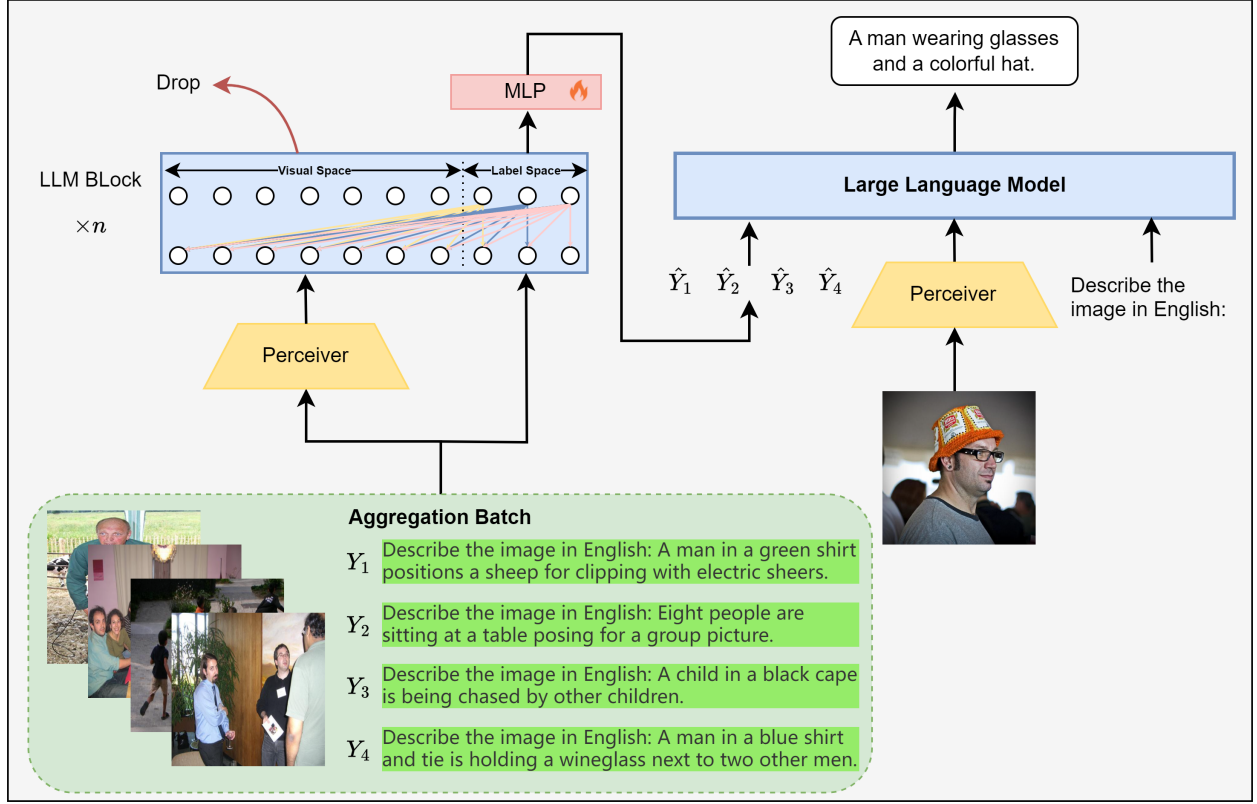


Figure 4: The architecture of AIM.  $Y_i$  is the  $i$ -th textual label of  $i$ -th image.

Table 1: Empirical comparison among recent MMLMs and AIM. ++ has a higher increase rate of memory cost/inference latency than +, as demonstrations increase.

Methods	In-context Learning Mode	Inner LLM	# Trainable Para.	Memory Costs ( $\Delta$ )	Inference Latency ( $\Delta$ )
Flamingo	multi-modal	Chinchilla	7B	Medium (+)	High (+)
MMICL	multi-modal	FLANT5-XXL	$\gg 17M$	Medium (++)	Low (++)
Qwen-VL	multi-modal	Qwen	7B	Medium (++)	Low (++)
LLaVA-Next	Language-only	Vicuna	7B	High (++)	Low (++)
AIM	multi-modal	ANY	17M	Low (+)	Medium (+)

space that the LLM can't understand directly, although it has fused with image information. We intuitively insert a learnable projection layer to convert  $H_i^Y$  into the LLM-acceptable fused tokens, similar to the perceiver converting visual features from vision encoder to visual tokens:

$$\hat{Y}_i = W_p \cdot H_i^Y, \quad (2)$$

where  $W_p$  is the parameters of the projection layer. Notably, aggregating image information of each image is independent of other demonstrations. Thus, AIM supports obtaining all  $\hat{Y}_i$  in a batch asynchronously or repeating this process for each demonstration synchronously to trade off memory costs with time.

Table 2: Details of involved evaluating datasets.

Dataset	Training	# Instances	Eval. Set	Eval.	Metric
Flickr30k	$\times$	1000	Test(Karpathy)	Open-Ended	CIDEr
OKVQA		5046	Val	Open-Ended	VQA acc.
Vizwiz		4319	Val	Open-Ended	VQA acc.
Hateful Memes		815	Seen Test	Cloese-Ended	ROC AUC

### 3.3 Response Generation in Multi-Modal ICL

AIM applies the entire frozen inner LLM to respond to current queries, with the guidance of our efficient demonstrations. For  $N$ -shot ICL, AIM obtains  $(\hat{Y}_1, \hat{Y}_2, \dots, \hat{Y}_N)$  independent from each

demonstration, concatenating them to configure an efficient demonstration sequence  $D = \hat{Y}_1 \oplus \hat{Y}_2 \oplus \dots \oplus \hat{Y}_N$ . Finally, the demonstration sequence  $D$  together with query image  $X_{query}$  and the prompt are fed into the inner LLM, performing auto-regressive generation:

$$y_t = \operatorname{argmax}(P(y|D; X_{query}; \text{ins.}; y_{<t})). \quad (3)$$

Additionally, we utilize closed-ended evaluation for understanding tasks by measuring AIM’s perplexity (PPL) among the label set. For a label sequence  $L = (l_1, l_2, \dots, l_m)$ , its PPL can be calculated as :

$$PPL(L) = \exp\left(-\frac{1}{m} \sum_{i=0}^m \log P(l_i|D; X_{query}; \text{ins.}; l_{<i})\right). \quad (4)$$

For a label set  $\mathcal{L} = \{L_1, L_2, \dots\}$ , AIM consider  $L_p$  as the current prediction if  $PPL(L_p)$  is the closest to 1.

### 3.4 Training

The trainable parameters in AIM are merely 17M originating from the projection layer  $W_p$ , and we utilize the language modeling loss to optimize it. We collect 56k instances from the web multi-image dataset MMC4. Each instance includes several images  $[X_1, X_2, \dots, X_K]$ , and each image corresponds to a most similar text  $[Y_1, Y_2, \dots, Y_K]$  assigned by existing ViT-L/14 in CLIP, constructing an interleaved image-text training instance. Additionally, we ensure each training instance has non-overlapping remaining texts and concatenate them, denoted as  $Y^R = Y_{K+1} \oplus Y_{K+2} \oplus \dots$ .

AIM first aggregates  $X_i$  to its corresponding text  $Y_i$ , obtaining  $\hat{Y}_i$ . Then, the language modeling loss can be formulated as:

$$\text{loss} = -\frac{1}{|Y^R|} \sum_{t=0}^m \log P(Y_t^R | \hat{Y}_1, \dots, \hat{Y}_K; Y_{<t}^R). \quad (5)$$

Notably, the carefully designed training approach separates the information aggregation of different images, breaking the inner relevance among images crawled from the same web page, increasing learning difficulty, and scaling up model robustness. Specifically, this gets rid of the influence of other image-text pairs, allowing each image to focus on the given text only and better match the patterns of ICL intuitively. Additionally, it brings AIM crucial merit that each aggregated result can be cached independently, formulating a demonstration bank (DB) for further reusing without aggregating image information into its latent space of demonstrated texts every time.

## 4 EXPERIMENT

### 4.1 Dataset

We briefly illustrate the involved dataset of AIM in Table 2. Involved evaluation datasets are filtered according to the mixture downstream training dataset of the underlying MLLMs to simulate the ICL scenario.

#### 4.1.1 Training Data.

*multi-modal C4*. MMC4<sup>2</sup> is a public open, billion-scale corpus of images interleaved with text. CLIP ViT-L/14 assigns each image with the most matched text crawled from the web. Due to AIM being trained parameter-efficiently, we merely utilize a subset of

<sup>2</sup><https://github.com/allenai/mmc4/tree/main>.

56k instances to formulate our training set, which contains 223k images and 1M texts.

#### 4.1.2 Evaluating Data.

*Flickr30k*. Flickr30k<sup>3</sup> [30] is a popular captioning dataset that contains 31,000 images collected from Flickr with 5 references annotated by humans.

*OKVQA*. OKVQA<sup>4</sup> [25], Outside Knowledge Visual Question Answering, includes over 14k manually filtered questions that require external knowledge, with 5 ground truth answers for each question respectively.

*Vizwiz*. Vizwiz<sup>5</sup> [11] dataset originates from a natural VQA setting where blind people each took an image and recorded a spoken question about it, together with 10 crowdsourced answers for each image. Especially, Vizwiz requires model responding “unanswerable” when the provided image is insufficient to answer the question.

*Hateful Memes*. Hateful Memes<sup>6</sup> [14] is a binary classification dataset to detect hateful speech in multi-modal memes. Their mentioned “Seen/Unseen” Test sets are distinguished by whether it is described in their paper or their challenge competition report.

### 4.2 Evaluation Metrics

We widely evaluate AIM on a spectrum of vision-language benchmarks, including Flickr30k, OKVQA, Vizwiz, and Hateful Memes. Following previous studies, we use CIDEr for Flickr30k, VQA-ACC for OKVQA and Vizwiz, and ROC AUC scores for Hateful Memes. All the evaluation scripts are publicly available on the repository of OpenFlamingo<sup>7</sup>.

### 4.3 Setting

During training, we set the maximum number of pictures to 5 per step for efficiency and filtered images if their similarities with all texts below 0.24 following OpenFlamingo. We fix the learning rate to 3e-5 and use Adam as the optimizer, and the effective batch size is 16 (4 GPUs data parallelism and 4 steps gradient accumulation). The number of epochs is set to 10 and we get a checkpoint per 3400 training steps. Additionally, we conduct all experiments on a single DGX node with 8\*Nvidia H800 GPUs. LLaVA-Next supports processing any resolution image by splitting it into sub-images, bringing several times visual tokens. We ignore this character and require LLaVA to pad each image to 336\*336 resolution since AIM introduces mass pictures as demonstrations<sup>8</sup>.

We borrow some crafted prompts from previous studies. For captioning, we format demonstrations as “[image] Describe the image in English in one sentence: [caption]”; For VQA we format demonstrations as “[image]\n[question] Answer in a word: [answer]”; For Hateful Memes, we prompt the model with “[image] is an image with [text] written on it. Is it hateful? Answer: [answer]”.

<sup>3</sup><http://nlp.cs.illinois.edu/Denotation.html>.

<sup>4</sup><https://okvqa.allenai.org>.

<sup>5</sup><https://vizwiz.org/tasks-and-datasets/vqa>.

<sup>6</sup><https://ai.meta.com/tools/hatefulmemes>.

<sup>7</sup>[https://github.com/mlfoundations/open\\_flamingo/tree/main/open\\_flamingo/eval](https://github.com/mlfoundations/open_flamingo/tree/main/open_flamingo/eval).

<sup>8</sup>Set image\_aspect\_ratio to pad.

**Table 3: Main results of AIM. *w/o visual* stands for providing textual label only. -16/24 represents the number of LLM layers applied to aggregate image information. † stands for the results from previous works and  $\bowtie$  indicates extra providing 2 textual label in 0-shot.**

Method	LLM	Flickr30k †					OKVQA †					Vizwiz †					Hateful Memes †									
		#-shots					#-shots					#-shots					#-shots									
		0	1	2	4	8	16	0	1	2	4	8	16	0	1	2	4	8	16	0	1	2	4	8	16	
Flamingo <sup>†</sup> $\bowtie$	Chinchilla (7B)	61.5	-	-	72.6	-	-	44.7	-	-	49.3	-	-	28.8	-	-	34.9	-	-	57.0	-	-	62.7	-	-	
Open Flamingo <sup>†</sup> $\bowtie$	MPT (7B)	39.2	-	-	52.2	58.7	60.6	38.3	-	-	42.0	44.1	45.1	34.6	-	-	41.0	45.0	46.2	67.1	-	-	70.1	71.2	73.2	
-Random <sup>†</sup> $\bowtie$		59.5	-	-	65.8	62.9	62.8	37.8	-	-	40.1	41.1	42.7	27.5	-	-	34.1	38.5	42.5	51.6	-	-	54.0	54.7	53.9	
Qwen-VL	Qwen (7B)	75.6	79.0	80.4	74.6	66.1	45.5	55.9	56.4	55.1	53.7	29.5	30.9	31.3	31.7	29.8	57.8	59.1	59.0	59.3	58.2					
-w/o visual		74.5	75.1	74.7	74.3	71.7	53.2	54.0	54.7	55.3	55.1	29.1	30.3	28.7	30.5	29.8	58.0	57.7	58.2	58.2	57.1					
AIM		74.3	67.6	76.2	78.1	78.8	82.3	55.3	55.6	55.4	55.8	56.1	56.0	28.4	<b>34.2</b>	34.3	35.1	35.6	36.1	58.3	<b>58.0</b>	<b>60.0</b>	57.8	58.9	57.1	
-16		55.1	<b>79.7</b>	<b>81.2</b>	<b>83.4</b>	<b>84.1</b>	<b>57.3</b>	<b>57.3</b>	<b>57.9</b>	<b>58.2</b>	<b>57.3</b>	30.9	<b>35.9</b>	37.6	<b>38.3</b>	<b>39.4</b>	55.6	56.4	<b>59.6</b>	<b>62.9</b>	<b>64.0</b>					
-24		63.9	74.4	73.3	75.8	78.1	56.2	56.6	55.2	54.3	53.5	31.8	34.2	34.3	34.6	34.6	52.5	57.1	56.9	57.4	59.1					
LLaVA-Next	Vicuna (7B)	<1	<1	<1	<1	<1	<1	<1	<1	<1	<1	16.4	14.0	11.2	<1	<1	53.6	54.7	55.6	NaN	NaN					
-w/o visual		47.2	47.7	48.1	47.6	44.3	51.2	52.6	52.9	51.5	52.8	21.1	20.6	21.7	20.5	19.9	56.1	56.5	55.9	55.6	55.0					
AIM		46.2	50.1	54.5	58.2	57.5	53.4	49.7	<b>54.0</b>	<b>55.1</b>	<b>55.3</b>	<b>55.0</b>	<b>54.6</b>	19.8	23.1	23.8	<b>24.1</b>	<b>21.5</b>	<b>20.2</b>	55.9	55.6	<b>56.6</b>	<b>58.6</b>	<b>57.8</b>	<b>55.6</b>	
-16		49.5	51.7	44.3	30.8	26.5	51.8	51.8	51.7	50.6	48.7	21.4	20.9	21.8	17.4	14.8	55.5	55.7	56.3	53.4	53.0					
-24		47.1	47.5	46.0	39.2	38.0	53.3	54.7	54.3	<b>55.0</b>	51.4	<b>23.3</b>	<b>23.8</b>	21.6	20.0	19.0	<b>55.7</b>	56.4	55.3	54.7	53.3					

Notably, following the previous studies [1, 2], we explicitly provide OCR text as inputs of AIM and baselines, and we don't extra prompt AIM can respond "unanswerable" in Vizwiz, reducing inappropriate induction.

#### 4.4 Baselines

Considering our aim to enable any MLLMs to embrace efficient ICL, the underlying backbones within AIM are convinced baselines to compare their efficiency and performance, namely, Qwen-VL and LLaVA-Next. We also cite the results of the comparative MLLMs from their published studies for reference:

- Flamingo: Similar to AIM, Flamingo, with the inner LLM having 7B parameters, breaks the quality between visual and textual modality and achieves outstanding performance on large-shot settings.
- OpenFlamingo: OpenFlamingo reproduces Flamingo in image-text tasks on the public dataset MMC4 which is also involved in the training set of AIM, with the inner LLM having 7B parameters.

Other MLLMs focus on multi-modal ICL such as Otter [16] and MMICL [46] due to **non-overlapped evaluation datasets** (Otter) and **different model sizes** (MMICL). Additionally, MMICL evaluates their performance up to 4-shot settings.

#### 4.5 Result

We filter the benchmarks occurring in the training of our selected backbones to simulate the practical in-context learning situation. Interestingly, when provided Qwen-VL with demonstrations including textual information merely (*w/o visual* in Table 3), it even outperforms the large shots situation provided both visual and textual. Additionally, Qwen-VL produces significant performance degradation in all 4 benchmarks when provided with over 8 demonstrations. This further highlights that treating visual and textual tokens equally limits MLLMs from exhibiting outstanding ICL performance, despite Qwen-VL reading multi-image prompts during training.

While AIM aggregates image information into its linguistic space before generation, the input format is close to prompts containing

a single query image, significantly bridging the modal gap and bringing stable performance gains in Table 3, despite examples randomly sampled. Additionally, the valuable merit artfully unlocks the ICL ability of MLLM, represented by LLaVA-Next, trained on the single image-text pair.

For vision language tasks involved in this spectrum, AIM outperforms backbones provided with concrete visual features that achieve +18 CIDEr gains in 16-shot in Flickr30k. While in the Vizwiz dataset, AIM exhibits relatively lower performance compared with other multi-modal ICL methods since we don't prompt AIM to output 'unanswerable', avoiding not solid short-cut answers. Notably, both OpenFlamingo and AIM employ MMC4 as the multi-image training set, but AIM, even applying LLaVA as the backbone, still achieves comparable or even outstanding performance via aggregating image information when provided with random<sup>9</sup> demonstrations (refer to the *Random* row).

Concentrating on LLaVA-based AIM, the fused tokens combined with image and text information seem noiseless for the inner Vicuna, while the naive backbone fails to generate normally provided with multi-modal demonstrations. Especially in the close-ended evaluation, perplexities concerning golden labels become NaN in 8- and 16-shot settings, occurring overflow while calculating PPL. However, LLaVA-based AIM successfully embraces ICL and achieves stable performance gains compared with providing text only across all 4 datasets.

#### 4.6 Case Study

We intuitively illustrate the 4/8/16-shot comparison between AIM and the corresponding backbone on Flickr30k in Figure 7. Generally, AIM, using both LLaVA-Next and Qwen-VL as the underlying MLLM, effectively responds to the query, with the guidance of fused tokens. In the 4-shot of naive LLaVA-Next, it misunderstands the reference demonstrations as "a collage of four separate photographs" Furthermore, LLaVA-Next fails to generate normally with the number of demonstrations increasing to 8. Qwen-VL correctly understands multi-modal demonstrations, but it still feels confused about understanding demonstrations, copying the inner structural

<sup>9</sup> *Open Flamingo and Flamingo* utilizes RICES (Retrieval-based In-Context Example Selection) to select demonstrations in latent space.

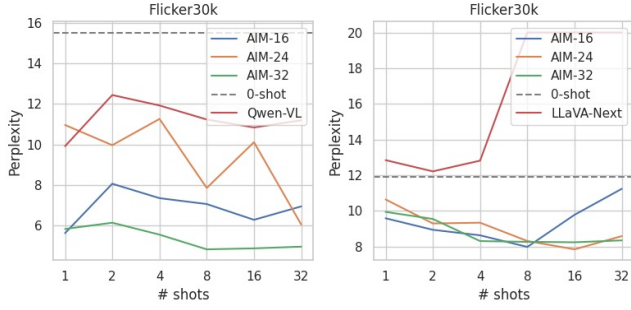


Figure 5: The perplexity variation tendency corresponds to the number of demonstrations. 0-shot server as the baseline.

format in the 4- and 8-shot settings. Additionally, the generated “Wall Street subway station” is not faithful to the query image in 16-shot settings.

## 5 ANALYSIS

### 5.1 LLM Layer Count for Aggregation

Considering the first layers directly interact with pre-trained embeddings, we perform ablation experiments on the first half, the first three-quarters to explore the number of LLM layers required to aggregate image information in Table 3. It is interesting that Qwen-VL prefers the first 16 layers, while LLaVA-Next is inclined to full layers being the aggregator. Therefore, the label words claim [36] that shallow layers (first half) focus on information aggregation is not completely applicable for LLaVA-Next in multi-modal settings.

From a posterior view, LLaVA-based AIM obtains stable performance gains with the aggregating layers become deeper. We attribute this conflict to LLaVA being pre-trained on single images, requiring deeper LLM layers to fuse image information into corresponding label space thoroughly, thus reducing the understanding difficulty for the built-in LLM. Additionally, The Connector in the LLaVA-Next project visual features from ViT to 576 visual tokens for a 336\*336 image, while Qwen-VL has 256 learnable queries. Therefore, LLaVA-based AIM requires deeper LLM layers to perform visual information gathering.

### 5.2 Perplexity Tendency of ICL

We briefly illustrate the perplexity variation tendency concerning golden labels of Flicker30k in Figure 5 with the number of demonstrations changing from 0 to 32 since Hateful Memes uses close-ended evaluation (the variation tendency of OKVQA and Vizwiz refer to Appendix). Notably, the perplexity blast occurring in both Qwen-VL and LLaVA-Next in the large shot setting indicates that the provided demonstration sequences significantly confused the underlying backbones, resulting in bad responses. While in the scope of AIM, the perplexity presents a decreasing tendency in general with some noise brought by randomly sampled demonstrations. Additionally, the most perplexity values are inferior to the 0-shot ones, indicating the provided demonstrations have a positive effect on helping MLLM generate current golden label responses.

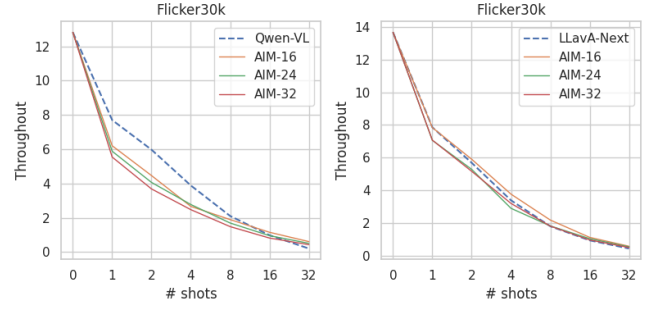


Figure 6: The throughput (iter/s) variation tendency is evaluated on a single H800, with the number of demonstrations increasing from 0 to 32.

Table 4: Quantity statistics of visual and textual tokens in multi-modal demonstrations.

Method	# Visual Tokens	Avg. Textual Tokens				Avg. Ratio
		Flickr30k	OKVQA	Vizwiz	Hateful Memes	
AIM-Qwen	256	30.1	16.0	15.7	29.3	8%
AIM-LLaVA	576	34.4	18.3	17.9	33.6	4%

### 5.3 Inference Throughput of AIM

AIM utilizes the inner LLM of existing MLLMs to complete image information aggregation operation. This character makes AIM not need to load the other “aggregator”, alleviating the memory costs. However, image information aggregation requires inevitable but minimal time costs due to the parallel computation of forward propagation. What’s more, AIM drops all the visual tokens after aggregating them into the dense label space, which compensates for aggregation time costs to some extent by reducing the input length during generation<sup>10</sup>. We evaluate the throughput (iter/s) of AIM on Flick30k in Figure 6 (The throughputs of OKVQA, Vizwiz, and Hateful Memes refer to Appendix).

Overall, in the few shot settings (less than 8), naive MLLMs are more efficient than AIM, but AIM has a lower inference latency increment. AIM becomes more efficient than the underlying backbone when provided with over 16 demonstrations.

### 5.4 Memory Cost of AIM

The normal attention mechanism is known as  $O(W^2)$  space complexity concerning a sequence with  $W$  words. Therefore, the length disaster brought by in-context demonstrations stimulates memory explosion straightforwardly. AIM drops the visual tokens after image information aggregation and the remaining ratios of fused tokens  $\mathcal{R}$  can be calculated according to the number of visual and textual tokens, denoted as  $|V|$  and  $|T|$ :

$$\mathcal{R} = \frac{|T|}{|V| + |T|}. \quad (6)$$

We demonstrate the quantity statistics over four datasets in Table 4, indicating that LLaVA-based AIM merely retains about 4% origin

<sup>10</sup>For Qwen-VL, AIM drops 256 visual tokens consistently, and AIM drops 576 visual tokens for a 336\*336 resolution image in LLaVA-Next.

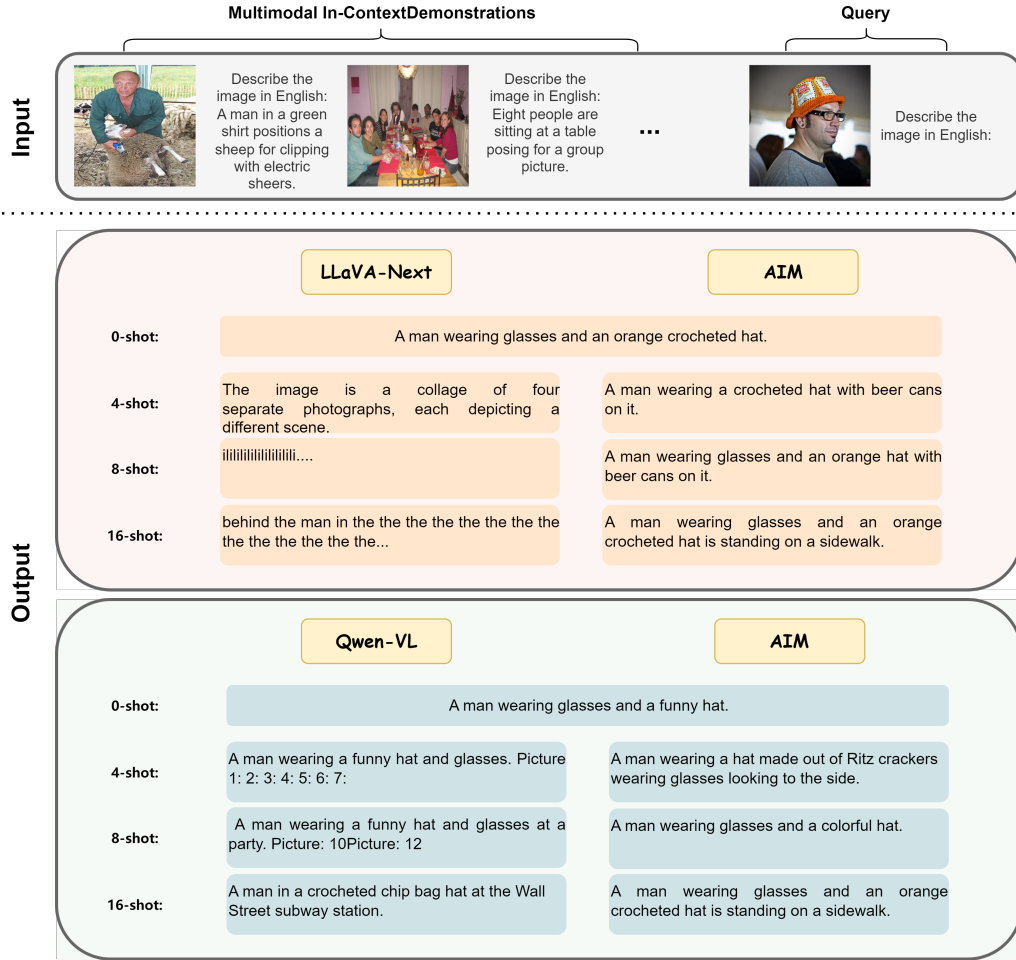


Figure 7: The case study of AIM and its two backbones on Flickr30k, the input is shared across all involved methods.

tokens in each multi-modal demonstration. Although LLaVA-Next integrates FlashAttention, dropping visual tokens still saves noticeable memory costs as illustrated in Figure 1. Notably, even if vision-language tasks have extremely long textual labels in assumption, AIM is capable of performing efficient ICL as normal with  $\mathcal{R}$  close to 1 since visual tokens have been dropped and the textual tokens are required anyway.

## 6 CONCLUSION

In this paper, our initial exploration delves into the attention distribution within the multi-modal ICL, revealing that the MLLM exhibits a greater emphasis on the linguistic modality. Built upon this discovery, we propose a light multi-modal framework AIM aiming to let any MLLMs embrace efficient ICL, which aggregates the image information of demonstrations into their dense latent space of demonstrated texts. Generally, AIM transforms the multi-modal ICL demonstration sequence into a form resembling a single query image accompanied by textual tokens. Thereby, AIM successfully coordinates with any MLLMs regardless of their initial support for

multi-modal ICL. Except for the outstanding performance of AIM compared with MLLMs specifically trained on multi-modal ICL, AIM is both training and inferencing efficient due to its frozen de facto backbone and dropping hundreds of visual tokens.

However, we think AIM still has a lot of room for improvement. For example, on the one hand, we are attempting to integrate the image information aggregation into the generation step, rather than separate it alone. On the other hand, RICES brought significant but not stable performance gains, we are curious about how to route these visual tokens, formulating a more suitable demonstration sequence.



## REFERENCES

- [1] Jean-Baptiste Alayrac, Jeff Donahue, Pauline Luc, Antoine Miech, Iain Barr, Yana Hasson, Karel Lenc, Arthur Mensch, Katherine Millican, Malcolm Reynolds, et al. 2022. Flamingo: a visual language model for few-shot learning. *Advances in neural information processing systems* 35 (2022), 23716–23736.
- [2] Anas Awadalla, Irena Gao, Josh Gardner, Jack Hessel, Yusuf Hanafy, Wanrong Zhu, Kalyani Marathe, Yonatan Bitton, Samir Gadre, Shiori Sagawa, et al. 2023. Openflamingo: An open-source framework for training large autoregressive vision-language models. *arXiv preprint arXiv:2308.01390* (2023).
- [3] Jinze Bai, Shuai Bai, Shusheng Yang, Shijie Wang, Sinan Tan, Peng Wang, Junyang Lin, Chang Zhou, and Jingren Zhou. 2023. Qwen-VL: A Frontier Large Vision-Language Model with Versatile Abilities. *arXiv preprint arXiv:2308.12966* (2023).
- [4] Daniel Bolya, Cheng-Yang Fu, Xiaoqi Dai, Peizhao Zhang, Christoph Feichtenhofer, and Judy Hoffman. 2022. Token merging: Your vit but faster. *arXiv preprint arXiv:2210.09461* (2022).
- [5] Tom Brown, Benjamin Mann, Nick Ryder, Melanie Subbiah, Jared D Kaplan, Prafulla Dhariwal, Arvind Neelakantan, Pranav Shyam, Girish Sastry, Amanda Askell, et al. 2020. Language models are few-shot learners. *Advances in neural information processing systems* 33 (2020), 1877–1901.
- [6] Alexis Chevalier, Alexander Wettig, Anirudh Ajith, and Danqi Chen. 2023. Adapting Language Models to Compress Contexts. *arXiv preprint arXiv:2305.14788* (2023).
- [7] Krzysztof Choromanski, Valerii Likhoshesterov, David Dohan, Xingyou Song, Andreea Gane, Tamas Sarlos, Peter Hawkins, Jared Davis, Afroz Mohiuddin, Lukasz Kaiser, et al. 2020. Rethinking attention with performers. *arXiv preprint arXiv:2009.14794* (2020).
- [8] Wenliang Dai, Junnan Li, Dongxu Li, Anthony Meng Huat Tiong, Junqi Zhao, Weisheng Wang, Boyang Li, Pascale N Fung, and Steven Hoi. 2024. Instruct-clip: Towards general-purpose vision-language models with instruction tuning. *Advances in Neural Information Processing Systems* 36 (2024).
- [9] Alexey Dosovitskiy, Lucas Beyer, Alexander Kolesnikov, Dirk Weissenborn, Xi-aohua Zhai, Thomas Unterthiner, Mostafa Dehghani, Matthias Minderer, Georg Heigold, Sylvain Gelly, et al. 2020. An image is worth 16x16 words: Transformers for image recognition at scale. *arXiv preprint arXiv:2010.11929* (2020).
- [10] Tao Ge, Jing Hu, Xun Wang, Si-Qing Chen, and Furu Wei. 2023. In-context Autoencoder for Context Compression in a Large Language Model. *arXiv preprint arXiv:2307.06945* (2023).
- [11] Danna Gurari, Qing Li, Abigale J Stangl, Anhong Guo, Chi Lin, Kristen Grauman, Jiebo Luo, and Jeffrey P Bigham. 2018. Vizwiz grand challenge: Answering visual questions from blind people. In *Proceedings of the IEEE conference on computer vision and pattern recognition*. 3608–3617.
- [12] Shaohan Huang, Li Dong, Wenhui Wang, Yaru Hao, Saksham Singhal, Shuming Ma, Tengchao Lv, Lei Cui, Owais Khan Mohammed, Barun Patra, et al. 2024. Language is not all you need: Aligning perception with language models. *Advances in Neural Information Processing Systems* 36 (2024).
- [13] Huiqiang Jiang, Qianhui Wu, Chin-Yew Lin, Yuqing Yang, and Lili Qiu. 2023. Llm-lingua: Compressing prompts for accelerated inference of large language models. *arXiv preprint arXiv:2310.05736* (2023).
- [14] Douwe Kiela, Hamed Firooz, Aravind Mohan, Vedanuj Goswami, Amanpreet Singh, Pratik Ringshia, and Davide Testuggine. 2020. The hateful memes challenge: Detecting hate speech in multimodal memes. *Advances in neural information processing systems* 33 (2020), 2611–2624.
- [15] Sehoon Kim, Sheng Shen, David Thorsley, Amir Gholami, Woosuk Kwon, Joseph Hassoun, and Kurt Keutzer. 2022. Learned token pruning for transformers. In *Proceedings of the 28th ACM SIGKDD Conference on Knowledge Discovery and Data Mining*. 784–794.
- [16] Bo Li, Yuanhan Zhang, Liangyu Chen, Jinghao Wang, Fanyi Pu, Jingkang Yang, Chunyuan Li, and Ziwei Liu. 2023. Mimic-it: Multi-modal in-context instruction tuning. *arXiv preprint arXiv:2306.05425* (2023).
- [17] Junnan Li, Dongxu Li, Silvio Savarese, and Steven Hoi. 2023. Blip-2: Bootstrapping language-image pre-training with frozen image encoders and large language models. *arXiv preprint arXiv:2301.12597* (2023).
- [18] Xiang Lisa Li and Percy Liang. 2021. Prefix-tuning: Optimizing continuous prompts for generation. *arXiv preprint arXiv:2101.00190* (2021).
- [19] Yucheng Li. 2023. Unlocking Context Constraints of LLMs: Enhancing Context Efficiency of LLMs with Self-Information-Based Content Filtering. *arXiv preprint arXiv:2304.12102* (2023).
- [20] Haotian Liu, Chunyuan Li, Yuheng Li, and Yong Jae Lee. 2023. Improved baselines with visual instruction tuning. *arXiv preprint arXiv:2310.03744* (2023).
- [21] Haotian Liu, Chunyuan Li, Yuheng Li, Bo Li, Yuanhan Zhang, Sheng Shen, and Yong Jae Lee. 2024. LLaVA-NeXT: Improved reasoning, OCR, and world knowledge. <https://llava-vl.github.io/blog/2024-01-30-llava-next/>
- [22] Haotian Liu, Chunyuan Li, Qingyang Wu, and Yong Jae Lee. 2024. Visual instruction tuning. *Advances in neural information processing systems* 36 (2024).
- [23] Zheheng Luo, Qianqian Xie, and Sophia Ananiadou. 2023. Chatgpt as a factual inconsistency evaluator for abstractive text summarization. *arXiv preprint arXiv:2303.15621* (2023).
- [24] Kenneth Marino, Mohammad Rastegari, Ali Farhadi, and Roozbeh Mottaghi. 2019. Ok-vqa: A visual question answering benchmark requiring external knowledge. In *Proceedings of the IEEE/cvpr conference on computer vision and pattern recognition*. 3195–3204.
- [25] Kenneth Marino, Mohammad Rastegari, Ali Farhadi, and Roozbeh Mottaghi. 2019. OK-VQA: A Visual Question Answering Benchmark Requiring External Knowledge. In *Conference on Computer Vision and Pattern Recognition (CVPR)*.
- [26] AI Meta. 2023. Introducing LLaMA: A foundational, 65-billion-parameter large language model. *Meta AI*. <https://ai.facebook.com/blog/large-language-model-llama-meta-ai> (2023).
- [27] Sewon Min, Mike Lewis, Hannaneh Hajishirzi, and Luke Zettlemoyer. 2022. Noisy Channel Language Model Prompting for Few-Shot Text Classification. In *Proceedings of the 60th Annual Meeting of the Association for Computational Linguistics (Volume 1: Long Papers)*. 5316–5330.
- [28] Jesse Mu, Xiang Lisa Li, and Noah Goodman. 2023. Learning to compress prompts with gist tokens. *arXiv preprint arXiv:2304.08467* (2023).
- [29] OpenAI. 2023. GPT-4 Technical Report. *arXiv:2303.08774 [cs.CL]*
- [30] Bryan A Plummer, Liwei Wang, Chris M Cervantes, Juan C Caicedo, Julia Hockenmaier, and Svetlana Lazebnik. 2015. Flickr30k entities: Collecting region-to-phrase correspondences for richer image-to-sentence models. In *Proceedings of the IEEE international conference on computer vision*. 2641–2649.
- [31] Alec Radford, Jong Wook Kim, Chris Hallacy, Aditya Ramesh, Gabriel Goh, Sandhini Agarwal, Girish Sastry, Amanda Askell, Pamela Mishkin, Jack Clark, et al. 2021. Learning transferable visual models from natural language supervision. In *International conference on machine learning*. PMLR, 8748–8763.
- [32] Hugo Touvron, Thibaut Lavril, Gautier Lzcard, Xavier Martinet, Marie-Anne Lachaux, Timothée Lacroix, Baptiste Rozière, Naman Goyal, Eric Hambro, Faisal Azhar, et al. 2023. Llama: Open and efficient foundation language models. *arXiv preprint arXiv:2302.13971* (2023).
- [33] Maria Tsimpoukelli, Jacob L Menick, Serkan Cabi, SM Eslami, Oriol Vinyals, and Felix Hill. 2021. Multimodal few-shot learning with frozen language models. *Advances in Neural Information Processing Systems* 34 (2021), 200–212.
- [34] Ashish Vaswani, Noam Shazeer, Niki Parmar, Jakob Uszkoreit, Llion Jones, Aidan N Gomez, Lukasz Kaiser, and Illia Polosukhin. 2017. Attention is all you need. *Advances in neural information processing systems* 30 (2017).
- [35] Jiaan Wang, Yunlong Liang, Fandong Meng, Haoxing Shi, Zhixu Li, Jinan Xu, Jianfeng Qu, and Jie Zhou. 2023. Is chatgpt a good nlg evaluator? a preliminary study. *arXiv preprint arXiv:2303.04048* (2023).
- [36] Lean Wang, Lei Li, Damai Dai, Deli Chen, Hao Zhou, Fandong Meng, Jie Zhou, and Xu Sun. 2023. Label Words are Anchors: An Information Flow Perspective for Understanding In-Context Learning. *arXiv preprint arXiv:2305.14160* (2023).
- [37] Zengzhi Wang, Qiming Xie, Zixiang Ding, Yi Feng, and Rui Xia. 2023. Is ChatGPT a good sentiment analyzer? A preliminary study. *arXiv preprint arXiv:2304.04339* (2023).
- [38] Jason Wei, Xuezhi Wang, Dale Schuurmans, Maarten Bosma, Ed Chi, Quoc Le, and Denny Zhou. 2022. Chain of thought prompting elicits reasoning in large language models. *arXiv preprint arXiv:2201.11903* (2022).
- [39] Xiang Wei, Xingyu Cui, Ning Cheng, Xiaobin Wang, Xin Zhang, Shen Huang, Pengjun Xie, Jinan Xu, Yufeng Chen, Meishan Zhang, et al. 2023. Zero-shot information extraction via chatting with chatgpt. *arXiv preprint arXiv:2302.10205* (2023).
- [40] David Wingate, Mohammad Shoeybi, and Taylor Sorensen. 2022. Prompt compression and contrastive conditioning for controllability and toxicity reduction in language models. *arXiv preprint arXiv:2210.03162* (2022).
- [41] Sang Michael Xie, Aditi Raghunathan, Percy Liang, and Tengyu Ma. 2021. An explanation of in-context learning as implicit bayesian inference. *arXiv preprint arXiv:2111.02080* (2021).
- [42] Xianjun Yang, Yan Li, Xinlu Zhang, Haifeng Chen, and Wei Cheng. 2023. Exploring the limits of chatgpt for query or aspect-based text summarization. *arXiv preprint arXiv:2302.08081* (2023).
- [43] Xu Yang, Yongliang Wu, Mingzhuo Yang, Haokun Chen, and Xin Geng. 2024. Exploring diverse in-context configurations for image captioning. *Advances in Neural Information Processing Systems* 36 (2024).
- [44] Pan Zhang, Xiaoyi Dong Bin Wang, Yuhang Cao, Chao Xu, Linke Ouyang, Zhiyuan Zhao, Shuangrui Ding, Songyang Zhang, Haodong Duan, Hang Yan, et al. 2023. Internlm-xcomposer: A vision-language large model for advanced text-image comprehension and composition. *arXiv preprint arXiv:2309.15112* (2023).
- [45] Renrui Zhang, Jiaming Han, Chris Liu, Peng Gao, Aojun Zhou, Xiangfei Hu, Shilin Yan, Pan Lu, Hongsheng Li, and Yu Qiao. 2023. Llama-adapter: Efficient fine-tuning of language models with zero-init attention. *arXiv preprint arXiv:2303.16199* (2023).
- [46] Haozhe Zhao, Zefan Cai, Shuzheng Si, Xiaoqian Ma, Kaikai An, Liang Chen, Zixuan Liu, Sheng Wang, Wenjuan Han, and Baobao Chang. 2023. Mmicl: Empowering vision-language model with multi-modal in-context learning. *arXiv preprint arXiv:2309.07915* (2023).
- [47] Wanrong Zhu, Jack Hessel, Anas Awadalla, Samir Yitzhak Gadre, Jesse Dodge, Alex Fang, Youngjae Yu, Ludwig Schmidt, William Yang Wang, and Yejin Choi.

ACM MM, 2024, Melbourne, Australia

Jun Gao<sup>\*1</sup>, Qian Qiao<sup>1</sup>, Ziqiang Cao<sup>1</sup>, Zili Wang, Wenjie Li<sup>2</sup>  
Institute of Artificial Intelligence, School of Computer Science and Technology, Soochow University<sup>1</sup>  
Department of Computer Science, Hong Kong Polytechnic University, Hong Kong<sup>2</sup>

2023. Multimodal C4: An Open, Billion-scale Corpus of Images Interleaved With

Text. *arXiv preprint arXiv:2304.06939* (2023).

# Supplementary Materials

## A INFORMATION FLOW

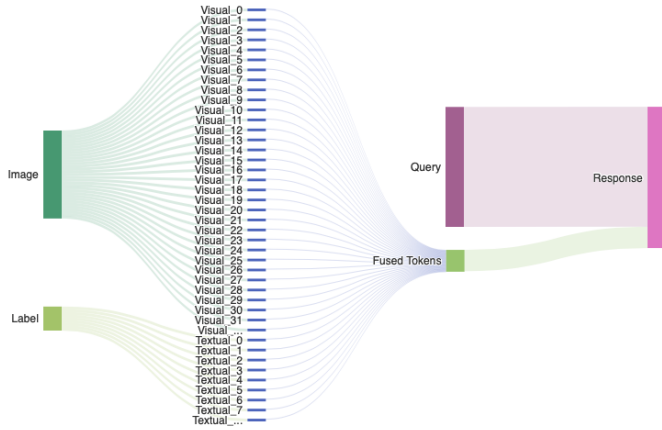


Figure 1: The information flow of How AIM performs image information aggregation (left) and response generation (right).

To better explain how AIM performs image information aggregation and response generation, we illustrate the information flow of AIM in Figure 1. Specifically, the image and labels derivate visual tokens and textual tokens, respectively, where the textual ones are much shorter than the visual ones. Then, AIM aggregates the visual information into dense latent space of labels through forward propagation that gets the last hidden states on top of the labels and converts them into fused tokens. Finally, fused tokens, serving as in-context demonstrations, together with the current query, are fed into the inner MLLM for response generation.

## B PERPLEXITY AND THROUGHPUT ANALYSES

Since Hateful Memes utilizes close-ended evaluation reflecting PPL implicitly, we provide the perplexity tendency on Flickr30k, OKVQA, and VizWiz in Figure 4, with the backbones of Qwen-VL and LLaVA-Next. Additionally, we demonstrate the throughput variation with respect to the number of demonstrations on Flickr30k, OKVQA, Vizwiz, and Hateful Memes in 5, with the backbones of Qwen-VL and LLaVA-Next.

## C TRAINING LOSS CURVE

We utilize Huggingface Trainer to optimize AIM for about 12 GPU hours on a single H800 node, with the default optimizer and scheduler. We demonstrate the training loss of AIM per 500 steps in Figure 2 and Figure 3.

## D LIMITATION AND DISCUSSION

Although AIM makes MLLMs embrace efficient ICL regardless of their backbone support reading multi-images initially, there are



Figure 2: Training loss curve of AIM, with Qwen-VL being backbone.

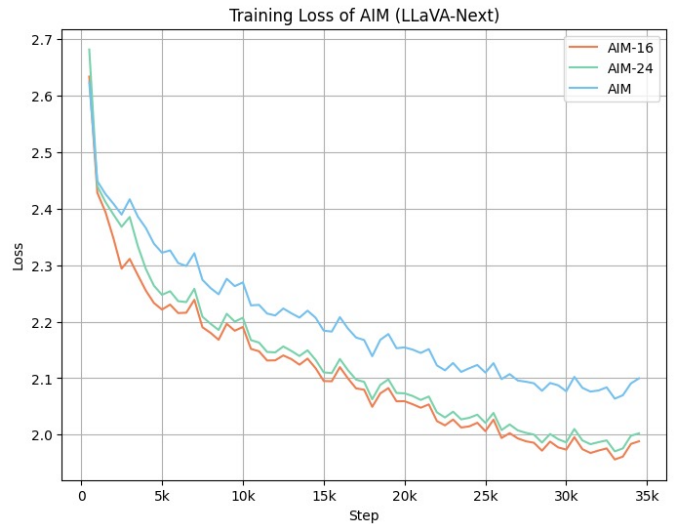


Figure 3: Training loss curve of AIM, with LLaVA-Next being backbone.

still limitations. The token remaining ratio in the original demonstration is determined according to the number of textual tokens, and therefore AIM will obtain less minimal efficiency gains if the labels are extremely over-length, despite the visual tokens being dropped and the textual tokens will exist anyway. Additionally, caching all demonstrations takes up a lot of storage space with the demonstrations increasing as well, and we are attempt to quantify the virtual demonstrations to allievate this problem.

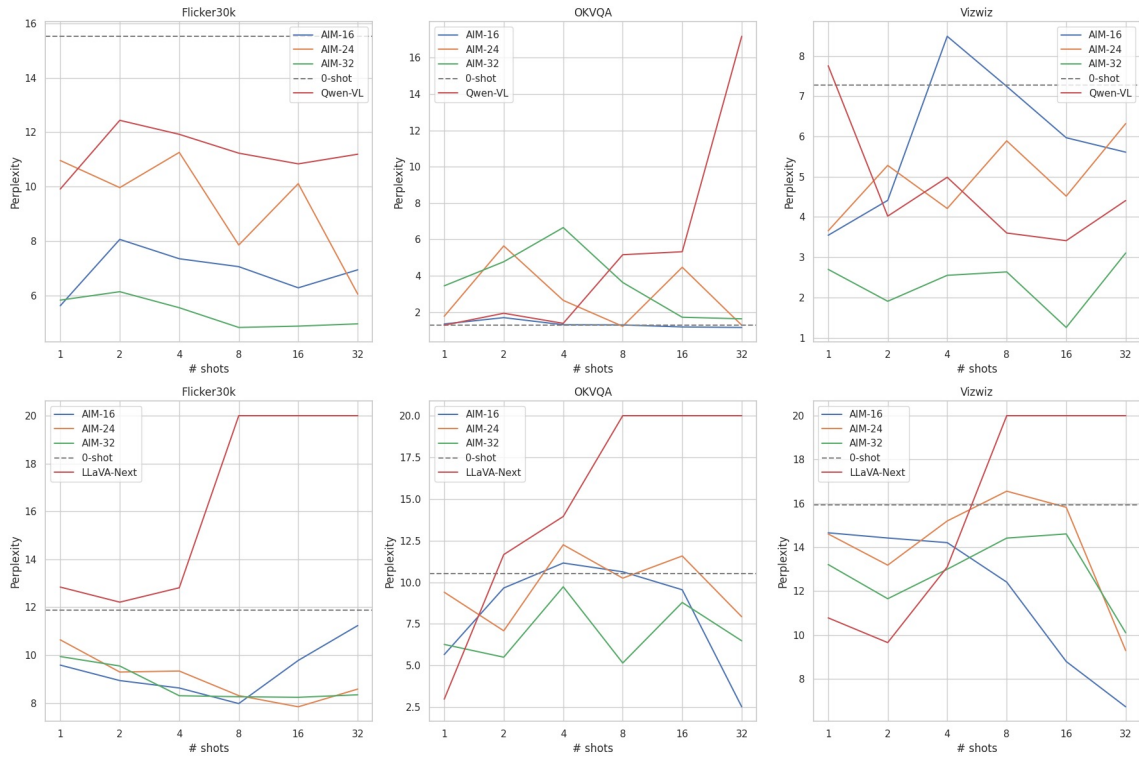


Figure 4: Perplexity analysis on Flickr30k, OKVQA and Vizwiz, with the backbone of Qwen-VL and LLaVA-Next.

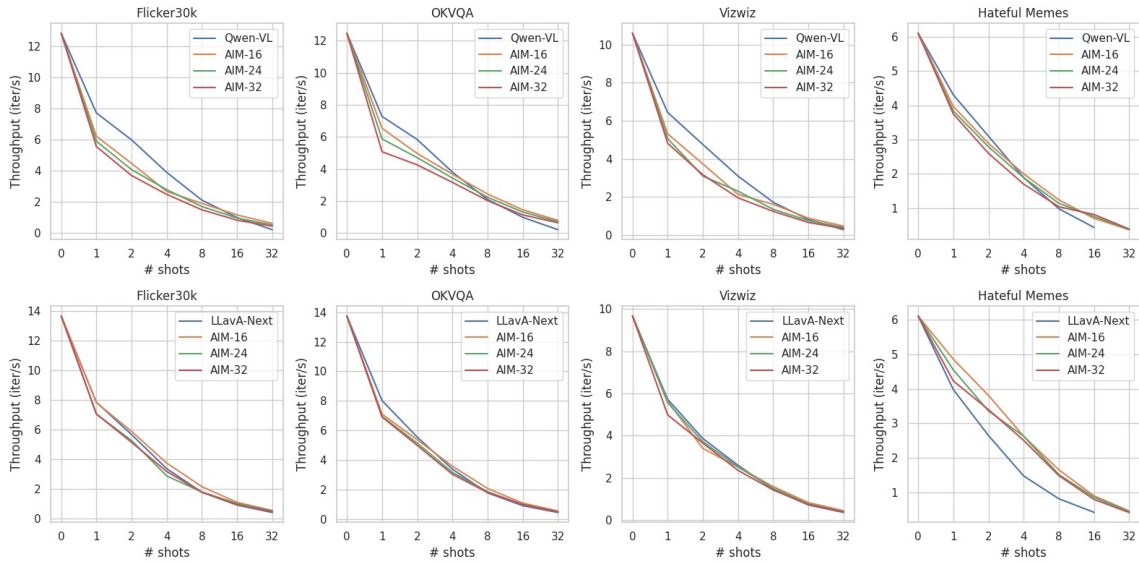


Figure 5: Throughput analysis on Flickr30k, OKVQA, Vizwiz and Hateful Memes, with the backbone of Qwen-VL and LLaVA-Next.